

Hydrazine solution-processed $\text{CuIn}(\text{Se},\text{S})_2$ thin film solar cells: Secondary phases and grain structure

Choong-Heui Chung^{a,b}, Brion Bob^a, Bao Lei^a, Sheng-Han Li^a, William W. Hou^a, Yang Yang^{a,*}

^a Department of Materials Science and Engineering and California NanoSystems Institute, University of California Los Angeles, Los Angeles, CA 90095, USA

^b Department of Materials Science and Engineering, Hanbat National University, Daejeon 305-719, Korea

ARTICLE INFO

Article history:

Received 2 October 2012

Received in revised form

31 December 2012

Accepted 16 February 2013

Available online 15 March 2013

Keywords:

Thin film solar cells

$\text{CuIn}(\text{Se},\text{S})_2$

Hydrazine

Secondary phases

Grain structure

ABSTRACT

We have carried out microstructural studies of secondary phase formation at the Mo/ $\text{CuIn}(\text{Se},\text{S})_2$ interface, and of grain structure in hydrazine solution-processed $\text{CuIn}(\text{Se},\text{S})_2$ films. The $\text{CuIn}(\text{Se},\text{S})_2$ layers were deposited on Mo-coated glasses followed by thermal annealing under a nitrogen ambient. In our previous work, we identified $[\text{Cu}_6\text{S}_4]^{2-}$ and $[\text{In}_2(\text{Se},\text{S})_4]^{2-}$ as the two major molecular species present in hydrazine $\text{CuIn}(\text{Se},\text{S})_2$ precursor solutions. The $\text{CuIn}(\text{Se},\text{S})_2$ films prepared by the precursor solution containing only above two molecular complexes exhibited the undesired secondary interfacial phases such as CuSe and CuIn_5S_8 . It is likely that the reactions between the Mo bottom electrode with sulfur in $[\text{Cu}_6\text{S}_4]^{2-}$ can result in the formation of a MoS_2 phase, triggering the phase separation of $\text{CuIn}(\text{Se},\text{S})_2$ into CuSe and CuIn_5S_8 . To make matters worse, the final $\text{CuIn}(\text{Se},\text{S})_2$ films contain a lot of voids that reduce the structural and electrical integrity of the device. The addition of polyselenide molecules $[\text{Se}]_n$ into the above $\text{CuIn}(\text{Se},\text{S})_2$ precursor solutions introduced MoSe_2 rather than MoS_2 at the back interface which in turn allows sulfur to remain in $[\text{Cu}_6\text{S}_4]^{2-}$ complexes. As a result, only the desired phases, $\text{CuIn}(\text{Se},\text{S})_2$ and MoSe_2 , were formed near the back interface. Furthermore, The formation of voids within the film can be also prevented by adding $[\text{Se}]_n$ into the $\text{CuIn}(\text{Se},\text{S})_2$ precursor solution, leading to the formation of a dense film structure.

© 2013 Elsevier B.V. All rights reserved.

1. Introduction

While crystalline silicon technology occupied approximately 85% of the photovoltaic market in 2010, these modules are still more expensive than fossil fuels largely because of the costly silicon wafers, impeding the wide-spread use of solar cells as an energy source [1]. Therefore, thin film solar cells, including cadmium telluride, copper chalcopyrite, polycrystalline silicon, and amorphous silicon have been extensively researched to reduce the fabrication cost of solar modules [2]. Among them, $\text{Cu}(\text{In},\text{Ga})(\text{Se},\text{S})_2$ solar cells have attracted a lot of attention due to their highest power conversion efficiency (PCE) of around 20% among thin film solar cells [3,4]. Achievement of such high PCE can be largely ascribed to the excellent optoelectronic properties of the absorber layer such as an Ohmic contact with the back electrode, long minority carrier life time, and optimized energy band gap. These desirable properties can be partially ascribed to the formation of a MoSe_2 phase at the Mo/absorber interface [5], large grain size in the absorber film [6], and partially replacement of indium and/or selenium by gallium and/or sulfur, respectively [3–6]. These properties are readily delivered by co-evaporation

techniques by precisely controlling the atomic flux of each element and the composition of film over the entire deposition period [3,4].

However, the use of vacuum facilities in the preparation of the absorber layer has still caused difficulty in the low-cost and large area production of solar modules. Therefore, a number of research efforts have been dedicated to the development of non-vacuum deposition methods for the preparation of the absorber layer in an effort to reduce the cost of producing these devices [7–12]. Almost all reported non-vacuum methods demonstrating reasonable PCE values require a post selenization and/or sulfurization step which typically uses vacuum facilities as well as toxic gases such as H_2Se and/or H_2S . Furthermore, an undesirable redistribution of indium, gallium, and sometimes sulfur upon post selenization/sulfurization makes it difficult to optimize the final energy band gap profile of the absorber layer.

Several years ago, Mitzi et al. developed hydrazine solution processed chalcogenide absorber layers including $\text{Cu}(\text{In},\text{Ga})\text{Se}_2$ (CIGS) and $\text{CuIn}(\text{Se},\text{S})_2$ (CISS) as a simple and high throughput process with no need for post selenization treatment [13–16]. Hydrazine processed CISS solar cells have been demonstrated with PCE values of 12.2% that are comparable to the record values of vacuum processed CuInS_2 , CuInSe_2 and $\text{CuIn}(\text{Se},\text{S})_2$ solar cells [14]. Furthermore, these hydrazine processed CIGS solar cells currently hold the highest published PCE value of 15.2% among

* Corresponding author. Tel.: +310 825 4052; fax: +310 825 3665.
E-mail address: yangy@ucla.edu (Y. Yang).

purely solution processed thin films solar cells despite its early stage of the development [16]. CIGS films used in the best solution-processed devices also exhibit a MoSe_2 phase at the Mo/CIGS interface, large grain size in the absorber film, and an adjustable energy band gap.

In our previous work, we reported hydrazine processed 7.4% efficiency CISS thin film solar cells [17]. In this study, we report microstructure formation mechanism of hydrazine solution-processed CISS films mainly aiming to understand secondary phase formation at the Mo/CISS interface and the resulting grain structure of the CISS films. In order to do this, we have directly probed secondary phases at the Mo/CISS interface using Raman spectroscopy and used scanning electron microscopy (SEM) to observe the grain structure of the CISS films. While $[\text{Cu}_6\text{S}_4]^{2-}$, and $[\text{In}_2\text{Se}_4]^{2-}$ are known to be two molecular complexes present in hydrazine CISS precursor solutions that are essential in forming the chalcopyrite CISS phase, the presence of excess selenium in the form of polymeric $[\text{Se}]_n$ structures appears to be vital to the fabrication of high efficiency photovoltaic devices. Here we focus on the role of polyselenide molecules $[\text{Se}]_n$ in achieving the desirable microstructure within the deposited CISS films including an analysis of MoSe_2 phase formation at the back interface as well as a dense CISS grain structure within the film itself. By optimizing microstructural properties of the CISS absorber layer based on the this information, we have demonstrated a roughly absolute 2% improvement in the PCE of hydrazine solution processed CISS thin films solar cells.

2. Experimental details

Photovoltaic devices with the structure $\text{MgF}_2/\text{Al}/\text{Ni}/\text{ITO}/\text{i-ZnO}/\text{CdS}/\text{CISS}/\text{Mo}/\text{Glass}$ were prepared on Mo-coated soda lime glasses by sequentially depositing the CISS absorber layer using hydrazine solution processing, the cadmium sulfide (CdS) buffer layer by chemical bath deposition, the bi-layered window layer consisting of intrinsic zinc oxide (i-ZnO) and indium tin oxide (ITO) by radio frequency sputtering, the bi-layered metal grid composed of nickel (Ni) and aluminum (Al) by thermal evaporation, and the magnesium fluoride (MgF_2) anti-reflection coating by thermal evaporation.

The CISS precursor solutions were prepared by mixing Cu-precursors containing Cu_2S and sulfur with In-precursors composed of In_2Se_3 and selenium and/or sulfur (Fig. 1). The details of solution precursor preparation can be found elsewhere [18,19].

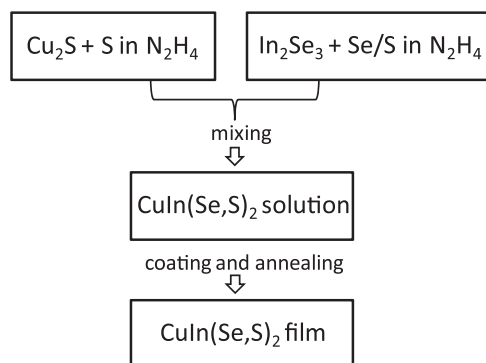


Fig. 1. Process flow for the preparation of hydrazine solution-processed $\text{CuIn}(\text{Se},\text{S})_2$ films. Cu-precursor solutions are prepared by dissolving Cu_2S and elemental sulfur in hydrazine, and In-precursor solutions are prepared by mixing In_2Se_3 with elemental selenium and/or sulfur in hydrazine. Two Cu-precursor and In-precursor solution are mixed with appropriate volume ratio to prepare final $\text{CuIn}(\text{Se},\text{S})_2$ precursor solutions. The resulting $\text{CuIn}(\text{Se},\text{S})_2$ films are prepared by spin-coating of the $\text{CuIn}(\text{Se},\text{S})_2$ precursor solutions followed by thermal annealing.

CISS films were deposited by spin-coating the hydrazine CISS precursor solutions at a spin-speed of 3000 rpm for 50 s. The coating was repeated to prepare $\sim 1.5 \mu\text{m}$ -thick layer to effectively absorb the solar spectrum. Between each coating step, the films were annealed at 300°C for several minutes, and finally annealed at 550°C for 15 min using rapid thermal annealing. *Caution: hydrazine is highly toxic and should be handled with appropriate protecting equipment to prevent contact with either the vapors or liquid.* The CdS layer was deposited from an aqueous bath containing cadmium acetate, thiourea, ammonium hydroxide and ammonium acetate at 65°C . The i-ZnO layer was deposited at a relatively mild sputtering condition with a deposition rate below $0.25 \text{ \AA}/\text{s}$ so as not to damage the devices. The ITO film was deposited at conditions of approximately 1% oxygen to argon working gas flow to achieve both high optical transmittance ($> 90\%$) and low sheet resistance ($\sim 35 \Omega/\text{sq}$).

Completed CISS films were mechanically exfoliated and flipped over onto 3 M tape. The images of exposed Mo surface and a flipped over CISS film were taken by optical microscope. Raman spectroscopy was performed on the prepared CISS films and the exposed Mo surface in a confocal backscattering configuration at room temperature using a Renishaw InVia model with a 514.5 nm argon laser as a light source.

The scanning electron microscope images were taken on a Jeol JSM-6700F electron microscope. The current density-voltage characteristics of the photovoltaic devices were measured using a Keithley 2400 power supply under a $100 \text{ mW}/\text{cm}^2$ simulated AM1.5G spectrum provided by an Oriel 91191 solar simulator.

3. Results and discussion

The presence of a thin layer of MoSe_2 at the Mo/absorber interface has been reported to provide Ohmic back contact which is important for achieving high performance photovoltaic devices [20]. MoSe_2 phase can be typically formed by flowing selenium vapor or H_2Se gas onto substrates held at temperatures above 400°C during or after growth of the absorber layers [4,21]. In the hydrazine solution process, absorber layers are generally deposited at room temperature followed by high temperature annealing under nitrogen ambient. In other words, this process does not contain a continuous flux of selenium vapor or molecules containing selenium impinging on the substrate while it is held at high temperature. Thus, molecular species containing selenium atom(s) in precursor solutions must be responsible for MoSe_2 phase formation.

$[\text{In}_2\text{Se}_4]^{2-}$, $[\text{Cu}_6\text{S}_4]^{2-}$, and polyselenide molecules $[\text{Se}]_n$ have been identified in hydrazine CISS precursor solutions [18]. We employed two different kinds of CISS precursor solutions for the study on microstructural properties of the resulting CISS films. One contains only two kinds of molecular species, $[\text{Cu}_6\text{S}_4]^{2-}$, and $[\text{In}_2\text{Se}_4]^{2-}$ which are essential to form CISS phase, and the other additionally contains polyselenide molecules $[\text{Se}]_n$ (Fig. 2). A pale yellow color and dark green color of the CISS precursor solutions originate from $[\text{Cu}_6\text{S}_4]^{2-}$ complexes, and polyselenide molecules $[\text{Se}]_n$ respectively.

In order to directly probe the microstructural properties of the prepared CISS films near the Mo surface, completed CISS films were mechanically exfoliated and flipped over onto 3 M tape (Fig. 3a). Fig. 3b and c show optical microscopy images of the exposed Mo surface and a flipped over CISS film on 3 M tape. Raman spectra were obtained from the exposed Mo surface, and the top and bottom surface of the CISS films marked as (1), (2) and (3), respectively, in Fig. 3 and Fig. 4.

In the CISS films prepared using CISS precursor solutions containing only the $[\text{Cu}_6\text{S}_4]^{2-}$ and $[\text{In}_2\text{Se}_4]^{2-}$ molecular complexes,

Download English Version:

<https://daneshyari.com/en/article/78276>

Download Persian Version:

<https://daneshyari.com/article/78276>

[Daneshyari.com](https://daneshyari.com)